Catalysis Science & Technology

Heterogeneous Pd complex catalyst for allylation with allylic alcohols enhanced by aluminum-doped mesoporous silica support

Journal:	*Catalysis Science & Technology*
Manuscript ID	CY-ART-10-2022-001768.R3
Article Type:	Paper
Date Submitted by the Author:	21-Feb-2023
Complete List of Authors:	Ding, Siming; Tokyo Institute of Technology, ; Yokohama National University, Department of Chemistry and Life Science Manaka, Yuichi; National Institute of Advanced Industrial Science and Technology, Renewable Energy Research Center; Tokyo Institute of Technology, School of Materials and Chemical Technology Nambo, Masayuki; Yokohama National University, Department of Chemistry and Life Science Chun, Wang-Jae; International Christian University, Graduate School of Arts and Sciences Tomita, Ikuyoshi; Tokyo Tech, Motokura, Ken; Yokohama National University, Department of Chemistry and Life Science; Tokyo Institute of Technology,

Heterogeneous Pd complex catalyst for allylation with allylic alcohols enhanced by aluminum-doped mesoporous silica support

Siming Ding,[a,b] Yuichi Manaka,[a,c] Masayuki Nambo,[b] Wang-Jae Chun,[d] Ikuyoshi Tomita,[a] Ken Motokura*[a,b]

[a] *Department of Chemical Science and Engineering, School of Materials and Chemical Technology, Tokyo Institute of Technology, 4259 Nagatsuta-cho, Midori-ku, Yokohama 226-8502, Japan*

[b] *Department of Chemistry and Life Science, Yokohama National University 79-5 Tokiwadai, Hodogaya-ku, Yokohama 240-8501, Japan. *E-mail: motokura-ken-xw@ynu.ac.jp*

[c] *Renewable Energy Research Center, National Institute of Advanced Industrial Science and Technology, 2-2-9 Machiikedai, Koriyama, Fukushima 963-0298, Japan*

[d] *Graduate School of Arts and Sciences, International Christian University, Mitaka, Tokyo 181-8585, Japan*

Abstract

Allylation using allylic alcohols is environmentally friendly because water is the only byproduct. Allylic alcohols are one of the most unreactive allylating agents for homogeneous Pd-catalyzed allylation; however, they can undergo electrophilic activation by acidic active species. Heterogeneous catalysts are known for their unique catalytic performance due to the

concerted effect of the immobilized metal center and support material surface. Our group has developed a mesoporous-silica-supported Pd complex catalyst that promotes the Tsuji–Trost allylation of dicarbonyl compounds with allylic alcohols through the concerted effect of Pd and surficial silanol groups. In this work, to enhance the catalytic activity of the supported Pd complex for allylation with allylic alcohols, the acidity of the support was increased by doping the silicate backbone with aluminum. Several spectroscopic techniques, such as Pd K-edge X-ray absorption fine structure (XAFS), solid-state NMR, and pyridine adsorption FT-IR measurements, were applied to confirm the structure of the catalyst. The Pd complex catalyst immobilized on the Al-doped support showed enhanced catalytic activity in allylation owing to the activation of the allylic alcohol by both the Al Lewis acid sites and silanol groups. The site-selective immobilization of the Pd complex through a silane-coupling reaction on Brönsted acid site (Si-O(H^+)-Al) enhances the concerted effect between the Pd complex and Lewis acidic Al site on MS surface.

1. Introduction

Since its discovery last century, Tsuji–Trost-type allylation has become a popular efficient synthetic method of constructing C–C bonds in the field of modern organic chemistry (Scheme 1(a)).[1] Among allylation approaches, the use of allylic alcohols as allylating reagents is welcome in the current research community because it can meet the demands of green chemistry, including water as the sole byproduct (Scheme 1(b)). Conventional homogeneous Pd catalysts, which have been studied worldwide for decades, are usually adopted in this reaction.[2] However, heterogeneous catalysts have attracted attention owing to their advantages in terms of reusability and separability especially in the field of chemical synthesis and waste water treatment. Both are sensitive to the residual amount of catalysts in the worked-up products. Moreover, immobilized metal complex catalysts exhibit a concerted effect from the support material, usually a polymer or silica, and the active metal center. Among them, polymer supporting materials were widely researched for their convenience of functionalization. Uozumi and co-workers made great efforts on cross-linking polymers of polystyrene-polyethylene glycol. Pd catalysts immobilized on such polymers gave high catalytic activities for allylation reaction.[3]

Nevertheless, polymers are also criticized by their hardness of degradation and consuming of petroleum feedstock. On the other hand, silica supports are known as their acidic surface and porous structure. More importantly, the abundant raw resources in lithosphere can easily exploited from crust of the earth. Silanol groups (Si-OH) on the surface of silica are versatile for immobilization, activation and structure modify. Mesoporous silica has a well-known benefit in large surface area, which increases the

reactivity by collision chances of reactants and surficial active sites. Organocatalysts such as amines immobilized on silica surface showed cooperative catalysis with surficial silanol groups by hydrogen bonding.[4] Our group has developed a mesoporous-silica-supported Pd complex catalyst that can catalyze the allylation of various nucleophiles with allylating agents and has a turnover number of up to 106000.[5] We demonstrated that active sites, for example, the Pd active center, silanol groups, and/or other functional organic groups, are accumulated in a tight mesopore space (Figure 1).[5f,g,h] In this way, allylic alcohols, which are thought to be unactivated and far less reactive than the normally used allylic halides, are activated by hydrogen bonding with silanol groups on the mesoporous silica surface. This concept of hydrogen-bonding activation of allylic alcohols has also been reported for homogeneous and heterogeneous systems.[6] The catalytic performance of the homogeneous Pd complex increased more than 8 times after the immobilization on mesoporous silica with surface silanol group.[5g]

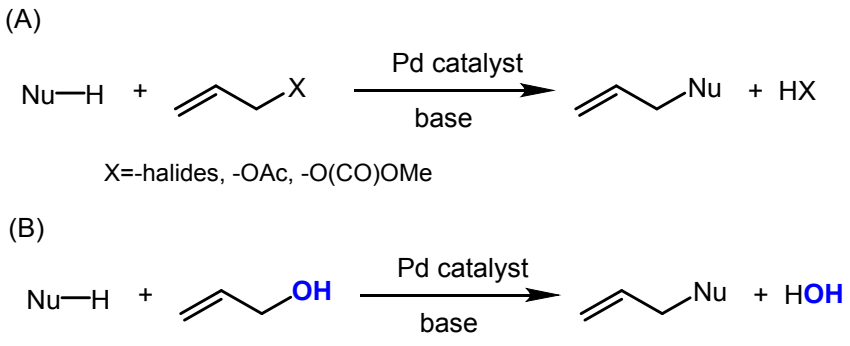

Scheme 1. Tsuji–Trost reaction using (A) conventional allylating agents and (B) allylic alcohols.

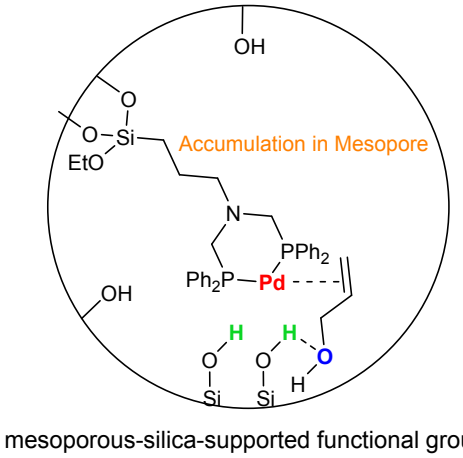

Figure 1. Dual activation of allylic alcohol by immobilized Pd complex and surface silanols.

The activity of this type of catalyst can be further enhanced through acidic activation of the support material. When aluminum is introduced into the mesoporous silica structural framework,[7] the tetrahedrally combined Al atoms are thought to contribute to the formation of both Lewis and Brønsted acid sites.[8] Cooperative catalysis between metal-doped mesoporous silica and surface amine group was reported by Jones and co-workers.[9] Herein, we fabricated a series of Pd bis(diphenylphosphine) complex catalysts supported on aluminum-doped mesoporous silica (MS-Al) and characterized their structural and surface properties using various spectroscopic methods. We focused on the influence of surface acidity which enhance the concerted activation effect on the Tsuji–Trost reaction with allylic alcohols (Scheme 2).

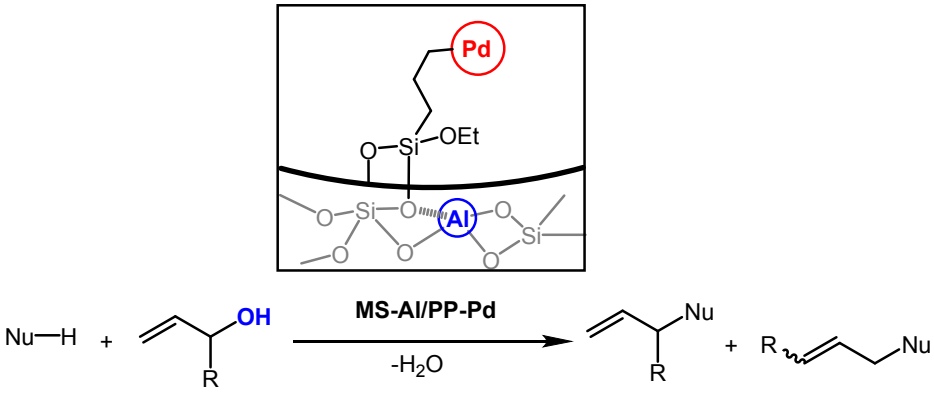

Scheme 2. The Tsuji-Trost reaction catalyzed by MS-Al/PP-Pd

Results and Discussion

2.1. Preparation and characterization of catalysts.

A series of aluminum-doped MCM-41 mesoporous silica (MS-Al) samples were synthesized through a well-known procedure using primary amines as the surfactants.[10] These structure-directing agents contain *n*-octylamine (C8), *n*-decylamine (C10), *n*-dodecylamine (C12), and *n*-octadecanamine (C18). The doping amount of aluminum in the precursor mixture is expressed as the Si:Al ratio X:1 (15:1, 30:1, and 75:1 in this work), and the corresponding samples are denoted as MS(Cn)-Al-X. The doping ratio can be controlled by adjusting the amount of $Al(OEt)_3$ introduced during the synthesis of MS-Al. As determined from the N_2 adsorption–desorption isotherms, MS(C8)-Al, MS(C10)-Al, MS(C12)-Al, and MS(C18)-Al had pore sizes of 1.3, 1.7, 2.1, and 2.6 nm, respectively, which are similar to those of undoped MS prepared using the same structure-directing primary amines.[5f-g,10]

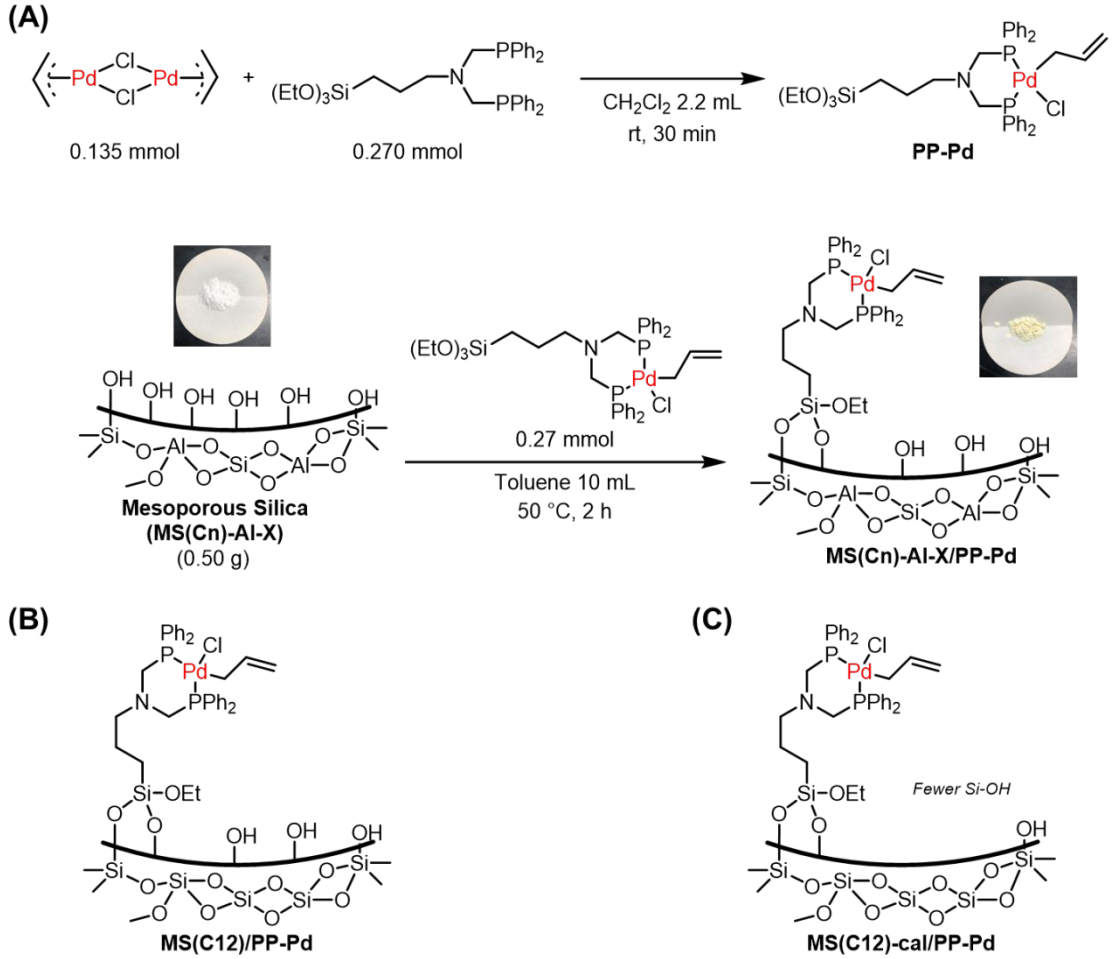

Scheme 3. (A) Synthesis of MS-Al-supported Pd complex catalyst, MS(Cn)-Al-X/PP-Pd. Structures of Al-free catalysts (B) MS(C12)/PP-Pd and (C) MS(C12)-cal/PP-Pd.

The synthesis of MS-Al/bis(diphenylphospine)Pd (PP-Pd) is illustrated in Scheme 3(A). The prepared PP-Pd precursor was treated with MS, which was first dried in vacuo for 3 h at 120 °C to remove the adsorbed surficial moisture, in toluene at 50 °C. Silane coupling afforded the corresponding supported catalysts, MS(Cn)-Al-X/PP-Pd. Formation of EtOH was detected in the liquid part after the immobilization. The amount of Pd was determined by inductively coupled plasma atomic emission spectroscopy (ICP-AES). The amount of Pd immobilized on catalysts were 3.6-4.1wt%. Detailed

elemental analysis results are summarized in Table S1(Supporting Information). For comparison, Pd catalysts supported on non-Al-doped MS with a pore size of 2.3 nm were also prepared (Schemes 3(B) and 3(C)). One of the support materials (MS(C12)cal) was calcined at 700 °C for 3 h and thus had fewer Si-OH groups on the surface.[11]

Figure 2 shows the energy dispersive X-ray spectrometry (EDS) mapping image of scanning electron microscope (SEM) of MS(C12)-Al-15/PP-Pd. The Si and Al mapping indicates the homogeneous doping distribution of Al atoms in the Si backbone. Pd and P mapping results also suggest that Pd species and phosphine ligand also highly dispersed on the support MS-Al surface. SEM-EDS images for other prepared samples for MS(C12)-Al-15, MS(C12)/PP-Pd and MS(C12)-cal/PP-Pd are shown in Supporting Information, Figure S1-S3, respectively.

Fourier transform infrared (FT-IR), solid-state nuclear magnetic resonance (NMR), and Pd K-edge X-ray absorption fine structure (XAFS) measurements were used to characterize chemical structure of the prepared supported catalysts. The FT-IR spectra of MS(C12)-Al-15 and MS(C12)-Al-15/PP-Pd are shown in Figure 3(A). The signals near 2900 and 1400 cm^{-1} were assigned to ν(C-H) and δ(C-H), respectively. The signal at 1437 cm^{-1} belonged to P-C bonds deformation band in P-CH_2-R group, while their stretching bands were located at 740 and 692 cm^{-1}. Signal of phenyl group of PP-Pd located near 1000 cm^{-1} was overlapped with Si-O-Si band.[12] The consumption of surface Si-OH by immobilization was confirmed by the ^{29}Si solid-state dipolar decoupling (DD) and cross-polarization (CP) magic-angle spinning (MAS) NMR spectra (Figure 3(B)). A strong signal at -100 ppm in CP/MAS NMR spectrum proved the existing of Si atom with hydrogen, indicating Q^3 [$Si(OH)_1(OSi)_3$] sites. The decreased

intensity of the signals at -91 and -100 ppm, which were assigned to Q^2 [$Si(OH)_2(OSi)_2$] (7.9%→5.8%) and Q^3 [$Si(OH)_1(OSi)_3$] (34.8%→29.8%) sites, respectively, illustrated the immobilization of PP-Pd. In addition, T sites with a signal at approximately -45 ppm were assigned to the silicon atom of the immobilized silane coupling reagent. This can also be observed clearly with higher intensity in CP/MAS NMR spectrum Figure 3(B).

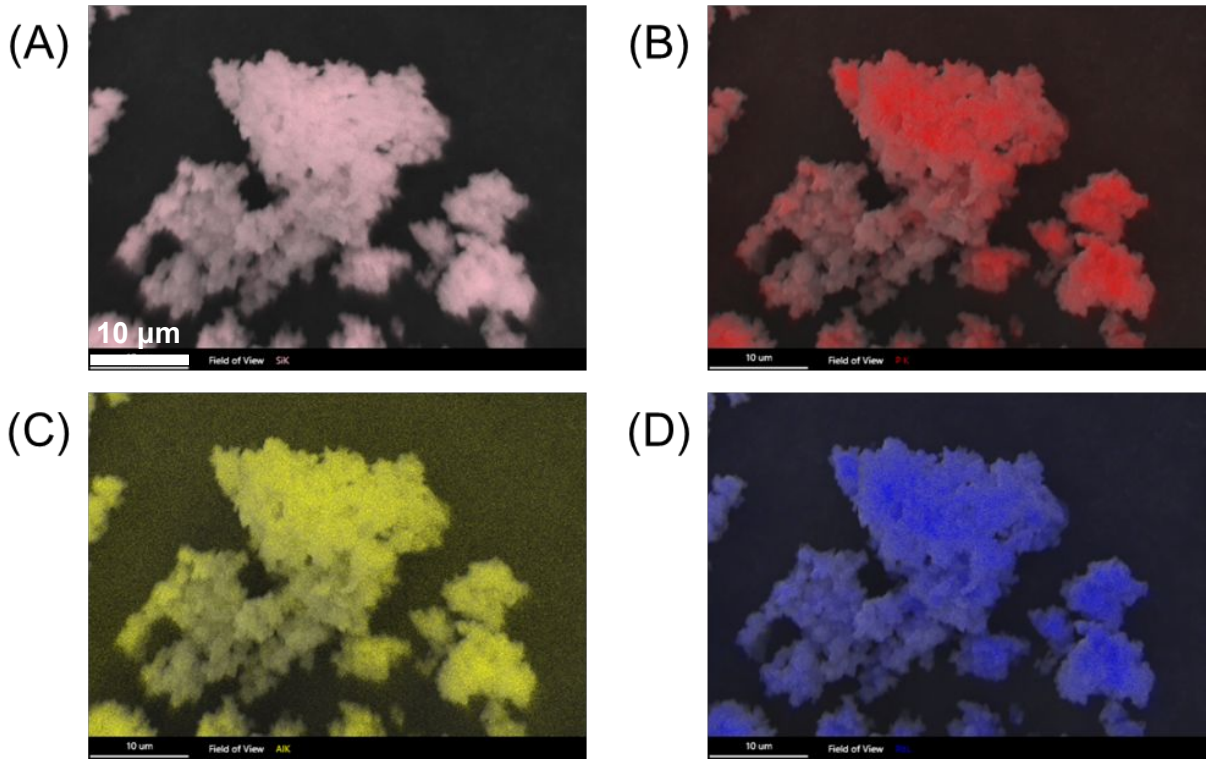

Figure 2. SEM-EDS mapping of MS(C12)-Al-15/PP-Pd for elements (A) Si, (B) P, (C) Al and (D) Pd.

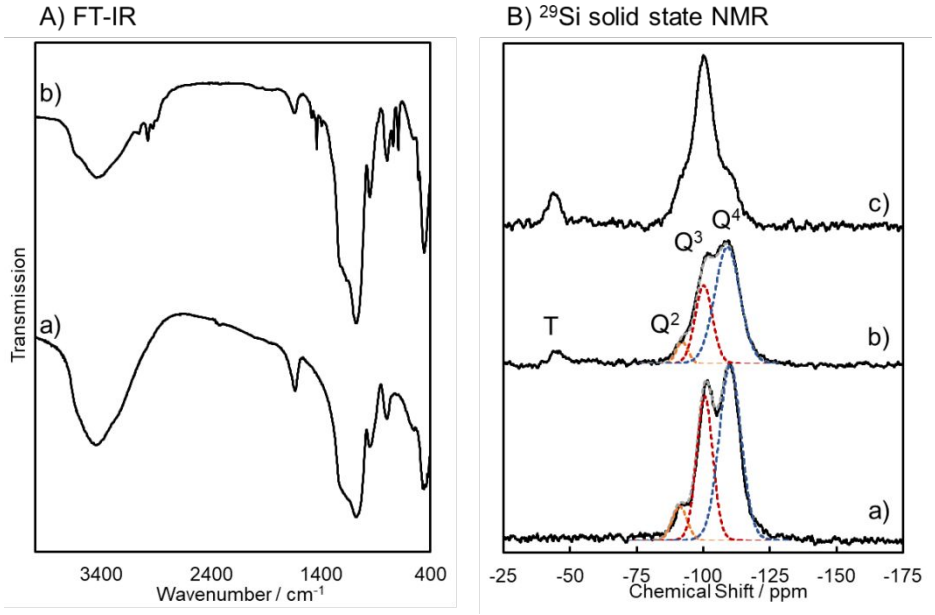

Figure 3. (A) FT-IR spectra of (a) MS(C12)-Al-15 and (b) MS(C12)-Al-15/PP-Pd (MS: mesoporous silica; MS-Al: Al-doped MS; PP-Pd: bis(diphenylphospine)Pd). (B) ^{29}Si solid-state MAS NMR of (a) MS(C12)-Al-15 (DD/MAS), (b) MS(C12)-Al-15/PP-Pd (DD/MAS), and (c) MS(C12)-Al-15/PP-Pd (CP/MAS). Separated signals from left to right are assigned to Q^2 (orange), Q^3 (red), and Q^4 (blue) sites.

The Pd K-edge X-ray absorption near edge structure (XANES) spectra (Figure 4(A)) showed that the shapes of the immobilized catalysts are similar to that of $PdCl_2(PPh_3)_2$, but much different from those of PdO and Pd(0) foil, indicating the monomeric complex structure of the Pd species after immobilization. Moreover, the Fourier transform of the extended X-ray absorption fine structure (FT-EXAFS) spectra of the supported Pd complexes, MS(C12)-Al-15/PP-Pd and MS(C12)/PP-Pd, showed a clear peak at 1.8 Å assigned to the Pd–P/Cl bonds (Figure 4(B)). The results of the curve-fitting analysis of the EXAFS spectra, summarized in Table 1, suggested that the PP-Pd precursor complex structure is maintained after immobilization on the MS support.

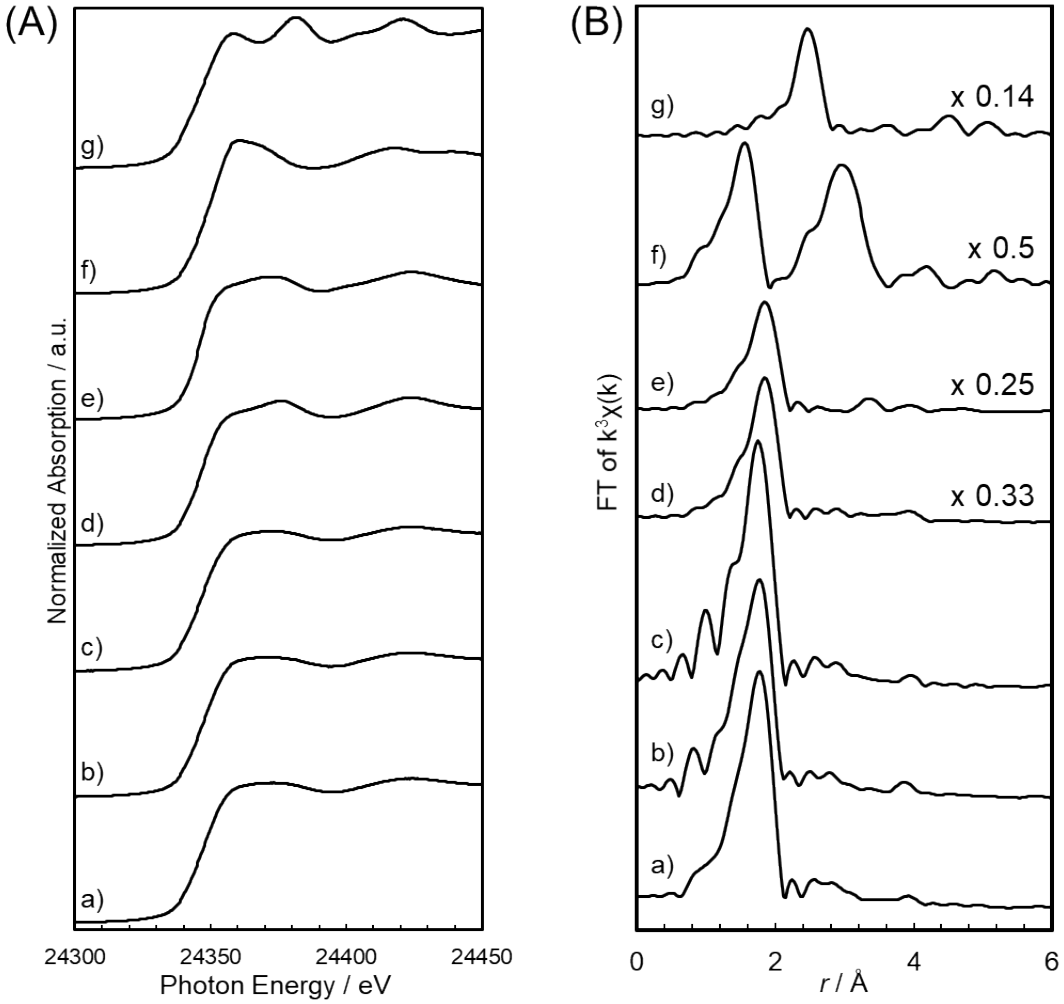

Figure 4. (A) Pd K-edge XANES spectra and (B) Fourier transform of k^3-weighted Pd K-edge EXAFS spectra of (a) MS(C12)-Al-15/PP-Pd, (b) MS(C12)/PP-Pd, (c) MS(C12)-cal/PP-Pd, (d) $PdCl_2(PPh_3)_2$, (e) $PdCl_2$, (f) PdO, and (g) Pd foil (Δk = 3–14 $Å^{-1}$).

Table 1. Curve-fitting analysis of the EXAFS spectra of fresh supported Pd catalysts with Pd-P/Cl shell.

Sample	Shell	N [b]	R (Å)[c]	DW factor[d] (Å)	ΔE_0 (eV) [e]	Rf (%)[f]
MS(C12)-Al-15/PP-Pd	Pd-P/Cl	3.0 (fixed)	2.28 ±0.01	0.08 ±0.01	-6.76 ±2.32	2.68
MS(C12)/PP-Pd	Pd-P/Cl	3.0 (fixed)	2.27 ±0.01	0.09 ±0.01	-5.61 ±2.33	4.00
MS(C12)-cal/PP-Pd	Pd-P/Cl	3.0 (fixed)	2.27 ±0.01	0.08 ±0.01	-6.87 ±2.32	1.82
$PdCl_2(PPh_3)_2$ [g]	Pd-P	2 (Pd-P)	2.34			
	Pd-Cl	2 (Pd-Cl)	2.30			

[a] Fourier transform and Fourier-filtering regions were limited, with $\Delta k \approx 3.0$–12 Å^{-1} and $\Delta r \approx$ 1.0–2.2 Å, respectively. [b] Coordination number. The coordination number of catalysts was fixed to 3 according to the former report,[5e] which contained 2 phosphine and 1 chloride coordination. [c] Bond distance between the absorber and backscattering atoms. [d] Debye (DW) factor relative to reference. [e] Inner potential correction to account for the difference between the inner potentials of the sample and reference. [f] Goodness of curve fit. [g] Reported average values of crystallographic data.[14]

The XANES, FT-EXAFS, and curve-fitting data for supported catalysts with different Al amounts and support pore sizes are shown in the Supporting Information (Figure S4 and Table S2). Conclusively, these characterization results prove that the amount of Al dopant or MS pore size has no effect on the immobilization mode.

The effect of Pd complex immobilization on the acid sites of the MS-Al surface was investigated by ^{27}Al MAS NMR and pyridine adsorption FT-IR spectroscopy. The ^{27}Al

single-pulse solid-state MAS NMR spectra of MS(C12)-Al-75 and MS(C12)-Al-75/PP-Pd (Figures 5(A) and (B)) exhibited two intense signals at approximately 57 and 11 ppm, which were assigned to tetracoordinate (tetrahedral) Al(IV) and hexacoordinate (octahedral) Al(VI) atoms, respectively.[13] This result indicates that tetrahedral Al(IV) maintains its structure during silane coupling immobilization.

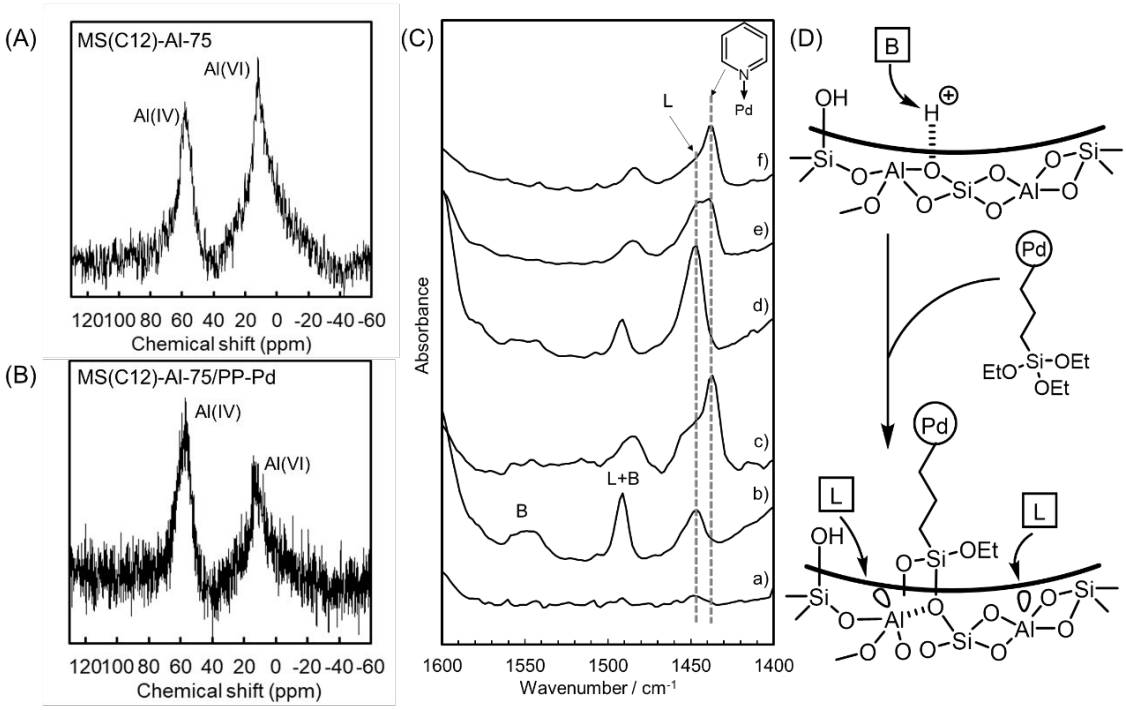

Figure 5. ^{27}Al NMR spectra of (A) MS(C12)-Al-75 and (B) MS(C12)-Al-75/PP-Pd. (C) FT-IR spectra after pyridine adsorption on (a) MS(C12), (b) MS(C12)-Al-15, (c) MS(C12)-Al-15/PP-Pd, (d) MS(C12)-Al-75, (e) MS(C12)-Al-75/PP-Pd, and (f) MS(C12)/PP-Pd. L and B represent Lewis and Brønsted acid sites, respectively. (D) Schematic illustration of Pd complex immobilization on MS-Al surface.

The surface acidity of MS-Al/PP-Pd was evaluated by pyridine adsorption FT-IR spectroscopy (Figure 5(C)). After the evacuation of excess pyridine, no clear signals were observed with pure silica, MS(C12), (a in Figure 5(C)), whereas several signals

appeared in the case of MS(C12)-Al-15 (b in Figure 5(C)). This indicates that the strong acid sites are due to the incorporated Al species. The signals at 1450 and 1550 cm^{-1} were assigned to pyridine adsorbed on the Lewis and Brønsted acid sites, respectively,[15] suggesting the presence of both Al^{IV} Lewis acid site[16] and Si-O(H^+)-Al^{IV} species on the MS-Al surface. After the immobilization of PP-Pd on MS-Al-15, the peak at 1550 cm^{-1} disappeared and a new signal at 1440 cm^{-1}, assigned to pyridine adsorbed on the Pd site, was detected (c in Figure 5(C)). The signal at 1450 cm^{-1}, assigned to the Al Lewis acid site, was still observed after PP-Pd immobilization (c in Figure 5(C)). A similar signal change was observed for MS(C12)-Al-75 and MS(C12)-Al-75/PP-Pd (d and e, respectively, in Figure 5(C)). These results clearly reveal the (i) preservation of Al Lewis acid sites and (ii) consumption of Brønsted acid sites after the immobilization of PP-Pd on MS-Al. While there were observable Brønsted acid sites before immobilization, they were hardly retained by the immobilized Pd catalysts. This indicates that Brønsted acid sites inevitably disappear during the silane coupling reaction owing to their higher reactivity compared with common silanol groups. The MS-Al/PP-Pd catalysts in this work possessed Lewis acidity but limited Brønsted acidity. The proposed PP-Pd immobilization process is illustrated in Figure 5(D). The PP-Pd was immobilized selectively on the strong Brønsted acid sites connected with Al^{IV} and the remaining Al^{IV} exhibited Lewis acidity, resulting the Pd complex and Lewis acidic Al^{IV} should be located in close proximity. The active site pairing may be effective for a concerted catalysis.

2.2. Catalytic Tsuji–Trost-type allylation.

The effect of aluminum doping on the concerted activation of allylic alcohol was examined in a reaction with ethyl 2-oxocyclopentanecarboxylate as the nucleophile. The reaction constants for different MS support materials are summarized in Figure 6. First-order plots are shown in Supporting Information Figure S7 and S8. MS(C12)-Al-15/PP-Pd-catalyzed allylation showed higher reactivity, in terms of rate constant (k = 4.61 × 10^{-4} s^{-1}), than MS(C12)/PP-Pd (3.79 × 10^{-4} s^{-1}) and MS(C12)cal/PP-Pd (3.18 × 10^{-4} s^{-1}). This indicates that the reactivity is affected by the surface acidity due to the Al site and silanol groups. With stronger surface acidity, the activation of allylic alcohol is more efficient, making it easier for the hydroxyl group of the allylic alcohol to leave. The pyridine adsorption experiments of the catalysts (Figure 5) suggested that this effect may be incited by both Si–OH and the Lewis acid site, which is the vacant orbital of Al^{IV}. The lone pair of electrons on the hydroxyl oxygen of the allylic alcohol interacts with the unoccupied orbital of Al, causing the departure of the hydroxyl group and formation of a cationic carbon center that is attacked by the nucleophile. To examine the effect of the doping amount of Al in MS, MS(C12)-Al-30/PP-Pd and MS(C12)-Al-75/PP-Pd were used for the catalytic allylation of the ketoester with allylic alcohol, giving k=4.68 × 10^{-4} s^{-1} and 4.28 × 10^{-4} s^{-1}, respectively. These results indicate that a Si:Al doping ratio of 30:1 is sufficient to enhance supported Pd catalysis.

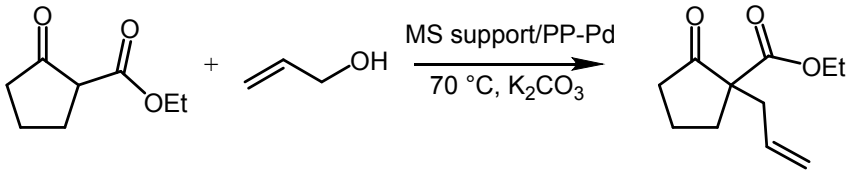

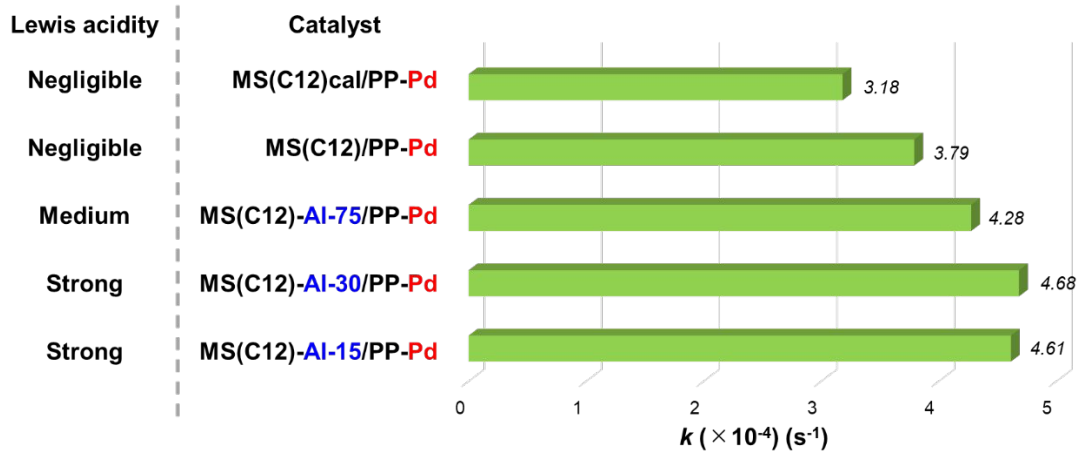

Figure 6. Allylation of ethyl 2-oxocyclopentanecarboxylate using allylic alcohol and 1-substituted allylic alcohols using MS supported PP-Pd catalysts. Reaction conditions: ethyl 2-oxocyclopentanecarboxylate (1.00 mmol), allylic alcohol (2.50 mmol), mesoporous silica (MS)-supported Pd catalyst (4 μmol), K_2CO_3 (0.50 mmol), neat, 70 °C. Lewis acidity was determined by pyridine-adsorbed FT-IR (1446 cm^{-1}).

To further study the effect of surface acidity, we used substituted allylic alcohols and catalysts with different surface acidities, namely MS(C12)-Al-15/PP-Pd, MS(C12)/PP-Pd, and MS(C12)cal/PP-Pd. The time course of the reaction and rate constant are summarized in Figures 7 and 8, respectively. First-order plots are shown in Supporting Information Figure S7-S10. There was a clear trend in the reactivities of the allylic alcohols with increasing surface acidity of the support material; specifically, the order of catalytic activity was MS(C12)-Al-15/PP-Pd > MS(C12)/PP-Pd > MS(C12)cal/PP-Pd. In addition, the reaction rate differences between the three catalysts became larger with an increase in the steric hindrance of the substituent (R). The reaction rate of allylic alcohol with ethyl group with Al-doped catalyst was 1.73 times higher than that of the catalyst without Al (Figure 8(B)). The main reasons are that (i) the surface acid site effectively activates allylic alcohols even with a sterically bulky group at the α-position, and (ii) the

electron-donating effect of the substituent (R) stabilizes the cationic carbon center formed with the assistance of surface acidity (Scheme 4). In this proposed mechanism, PP-Pd was firstly reduced by base, K_2CO_3 in this work, to form a Pd(0) active center. Then, the allylic alcohols were activated by surface acid sites and attacked by the Pd(0) center, affording a π-allyl Pd intermediate in the catalytic circle.[5d] Unfortunately, even with the MS-Al/PP-Pd catalyst, the reaction of 2-methyl-3-buten-2-ol and (*E*)-1,3-diphenyl-2-propen-1-ol proceeded with difficulty because of the large steric hindrance during activation. For γ-substituted allylic alcohols, crotyl alcohol gave 57% yield with 2-phenylpropionaldehyde under the catalysis of MS(C12)-Al-15/PP-Pd for 3 hours at 50 °C, while the 1-butene-3-ol gave only 11% yield under the same condition because of the steric hindrance at α-carbon.

Regarding final product yield, the Al-doped catalyst showed higher performance than simple MS-supported catalyst without Al. The Al-doped catalyst showed higher performance in the reaction of substituted allylic alcohols, especially. For example, in Figure 7, yield at 180 min for the reaction of 3-buten-2-ol (R=Me) was 72% (MS-Al/PP-Pd) and 62% (MS/PP-Pd). The yield with MS-Al/PP-Pd increased to 89% for 17 h. In the case of 1-penten-3-ol (R=Et), the final yield after prolonged reaction time for 17 h was 80% (MS-Al/PP-Pd) and 74% (MS/PP-Pd). These results clearly indicates that the final results using newly developed, Al-doped catalysts is superior to previously reported MS/PP-Pd (without Al) catalyst.

Allyl chloride, which is conventionally thought to be a reactive leaving group in homogeneous systems, gave poor yields with 2-phenylpropionaldehyde as a nucleophile

(25% yield with MS(C12)-Al-15/PP-Pd), while the allylic alcohol showed good reactivity in the supported Pd system (92% yield). This result also demonstrates the enhancement of reactivity by acid sites and/or silanol groups on the support surface, which activate the allylic alcohol and facilitates the departure of the hydroxyl group.[6]

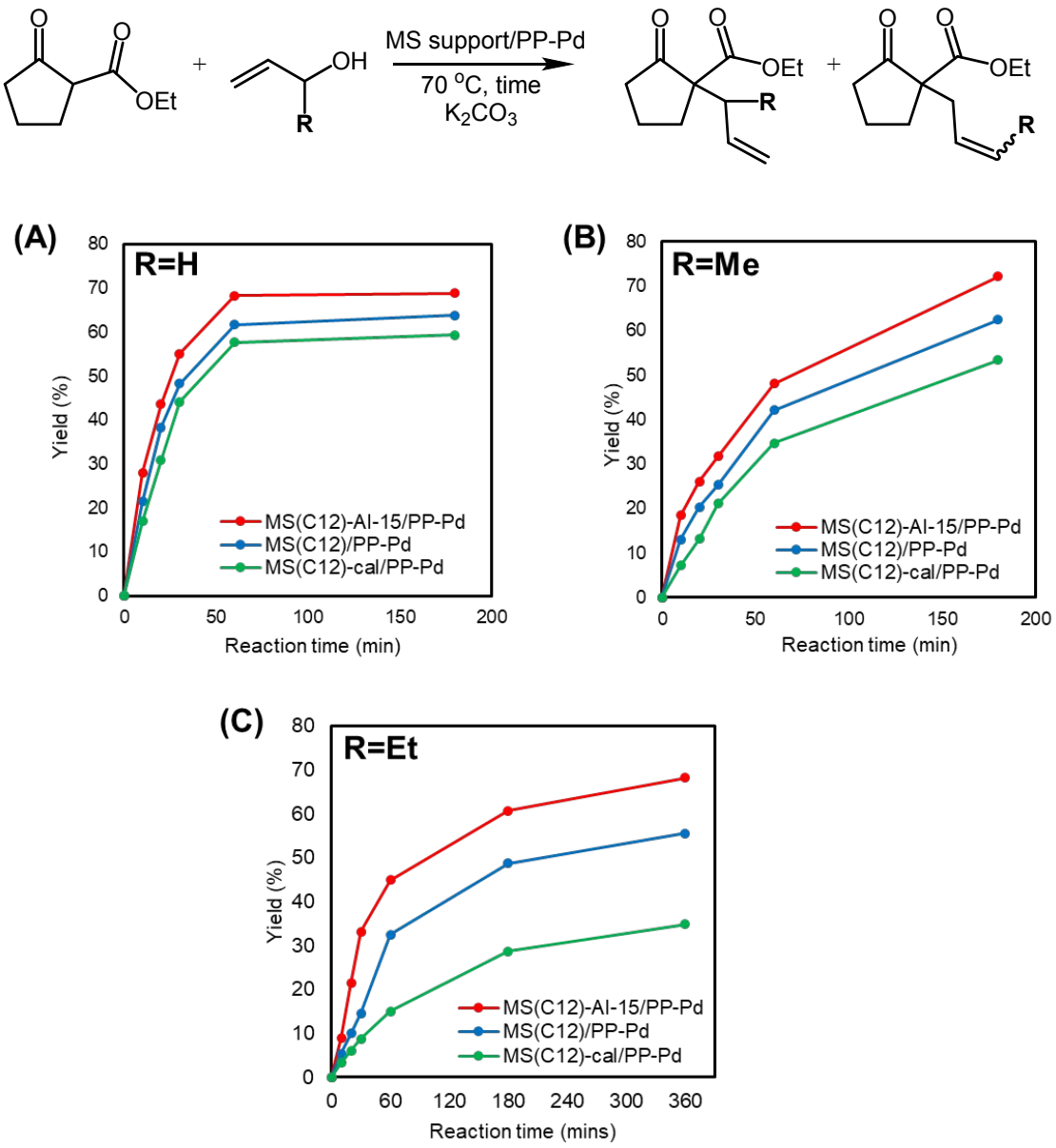

Figure 7. Time course of allylation of ethyl 2-oxocyclopentanecarboxylate using allylic alcohol and 1-substituted allylic alcohols. (A) R = H: nucleophile (1.00 mmol), allylic alcohol (2.50 mmol), mesoporous silica (MS)-supported Pd catalyst (4 μmol), K_2CO_3 (0.50 mmol), neat, 70 °C. (B) R = Me: nucleophile (1.00 mmol), 3-butene-2-ol (2.50 mmol), MS-supported Pd catalyst (8 μmol), K_2CO_3 (0.50 mmol), neat, 70 °C. Isomer ratio of product was almost same during the catalytic reactions in each catalytic reaction (*trans* : *cis* : branch = 62 : 17 : 21). (C) R = Et: nucleophile (1.00 mmol), 1-penten-3-ol (2.50 mmol), MS-supported Pd catalyst (12 μmol), K_2CO_3 (0.54 mmol), neat, 70 °C. Only *trans* product formed in each catalytic reaction.

(A)

Catalyst	Lewis acidity (1446 cm^{-1})	k ($\times 10^{-4}$) (s^{-1})		
		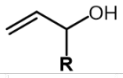		
		R=H	Me	Et
MS(C12)-Al-15/PP-Pd	Strong	4.61	2.33	1.79
MS(C12)/PP-Pd	Negligible	3.79	1.59	1.03
MS(C12)cal/PP-Pd	Negligible	3.18	1.21	0.47

(B)

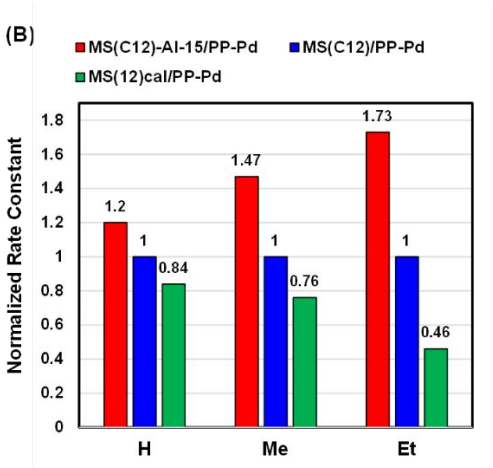

Figure 8. (A) Lewis acidity of catalysts determined by pyridine-adsorbed FT-IR (Figure 5) and rate constants of allylation with different substituted allylic alcohols and (B) their normalized values (MS: mesoporous silica; MS-Al: Al-doped MS; PP-Pd: bis(diphenylphospine) Pd). Reaction conditions are shown in Figure 7.

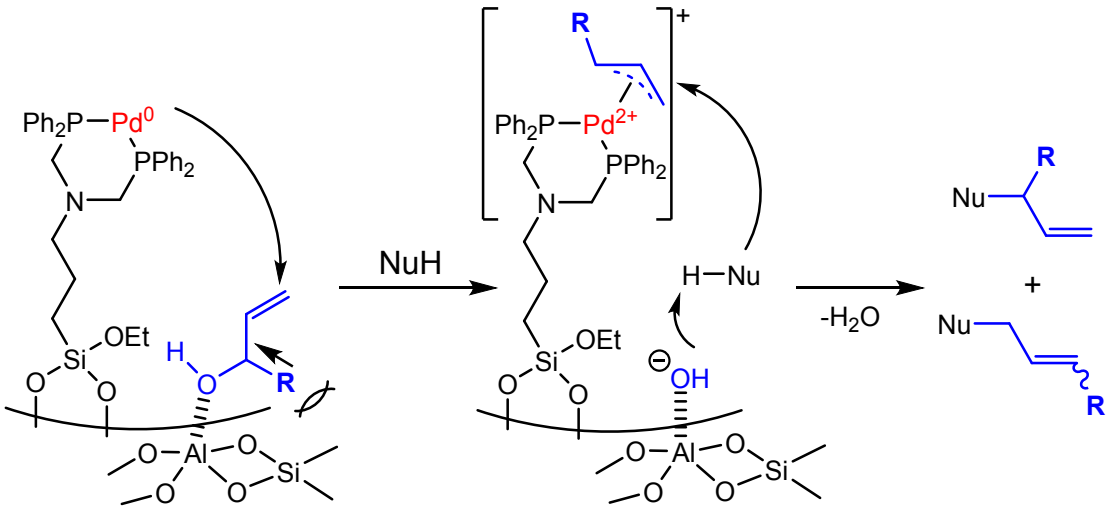

Scheme 4. Proposed activation mechanism of allylic alcohol during allylation.

Another factor is the pore size of the support material. MS(C12)-Al-15/PP-Pd afforded the highest yield (75%) in the catalytic allylation of 2-phenylpropionaldehyde

with allylic alcohol, while similar product yields were obtained when using MS(C10)-Al-15/PP-Pd (71%) and MS(C18)-Al-15/PP-Pd (71%) (Figure 9). The product yield slightly decreased with MS(C8)-Al-15/PP-Pd (62%). In MS-Al, the allylic alcohol is initially activated by Al Lewis acid sites on the surface and then attacked by the Pd center (Scheme 4). Because of the site-selective immobilization of PP-Pd on MS-Al, an almost same local environment of Pd complex-Lewis acidic Al should be constructed in all MS-Al materials. Therefore, the catalytic activity was not changed significantly when using MS(C10) to MS(C18). On the other hand, a very small pore size allows less reactant to enter the pore, leading to lower reactivity.[5f]

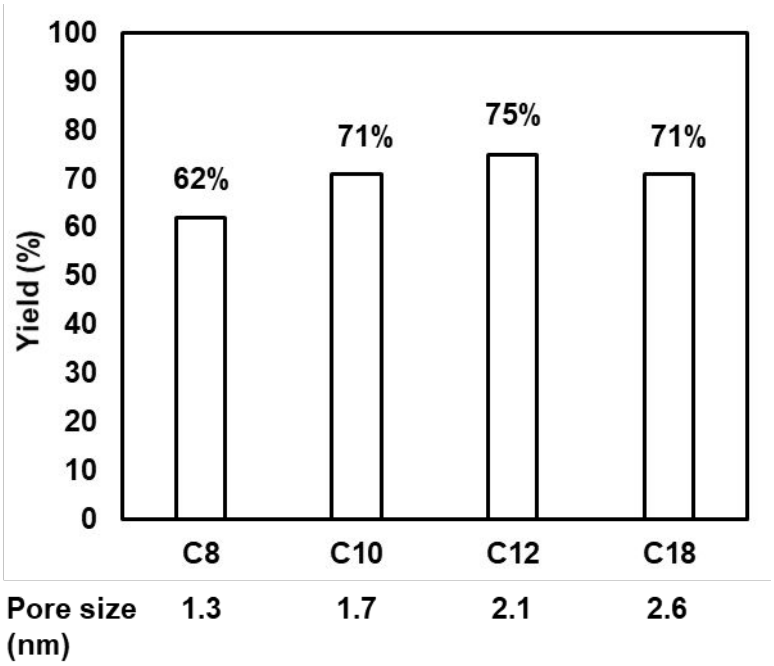

Figure 9. Effect of the pore size of Al-doped mesoporous silica [MS(C8)-Al~MS(C18)-Al] on the yield of allylation with allylic alcohol. Reaction conditions: 2-phenylpropionaldehyde (1.00 mmol), allylic alcohol (2.50 mmol), MS(Cn)-Al-15/PP-Pd (8 μmol), K_2CO_3 (0.50 mmol), neat, 3 h, 70 °C.

Table 2. Scope of nucleophiles for allylation reaction catalyzed by MS(C12)-Al-15/PP-Pd.[a]

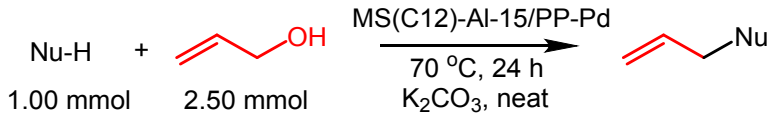

Entry[a]	Nu-H	Yield(mono/di) [%]
1	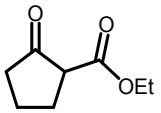	82 [85[c],68[d]]
2[b]	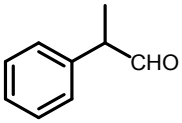	92
3	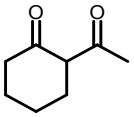	49
4	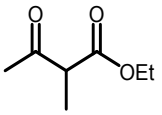	57
5	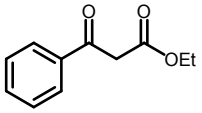	62 (32/30)
6	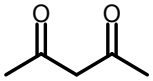	70 (12/58)
7	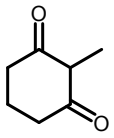	70
8	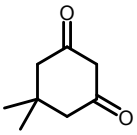	79 (2/77)

[a] Reaction conditions: MS(C12)-Al-15/PP-Pd (8.0 μmol), nucleophile (1.00 mmol), allylic alcohol (2.50 mmol), K_2CO_3 (0.50 mmol), neat, 24 h, 70 °C; [b] MS(C12)-Al-15/PP-Pd (8.0 μmol), nucleophile (1.00 mmol), allylic alcohol (2.50 mmol), K_2CO_3 (0.50 mmol), neat, 24 h, 50 °C. [c] 2nd use, [d] 3rd use.

The scope of the nucleophile substrates is shown in Table 2. The reactions were performed using 1.0 mmol of nucleophile and 8 mol% (8.0 μmol) of Pd in the MS(C12)-Al-15/PP-Pd catalyst under solvent-free conditions. Acyclic, cyclic, and aromatic ketoesters and diketones reacted with allylic alcohol to give the corresponding allylation products in up to 82% yield. The catalyst was reused three times, and the reactivity was maintained at 85% and 68% yield for the 2nd and 3rd uses, respectively. Leaching of the MS(C12)-Al-15/PP-Pd catalyst was investigated by hot filtration experiment. The catalyst was separated after 5 min of reaction, and the fraction without the catalyst did not undergo further reaction (Figure S11, Supporting Information). This indicates that leaching did not occur during the catalytic reaction. As a support, the ICP test of Pd content in the liquid from reaction mixture gave the result below the detection limit.

Summary

In this study, a series of Pd complex catalysts supported on aluminum-doped mesoporous silica (MS-Al/PP-Pd) were synthesized and characterized. The catalytic activation of the immobilized catalysts toward the Tsuji–Trost-type allylation of 2-phenylpropionaldehyde achieved a yield of up to 92% with allylic alcohol, the most efficient and green leaving group under neat conditions. The reaction was catalyzed by the concerted effect of the Lewis acid and activation of allylic alcohol via hydrogen bonding with silanol groups on the support material. Increasing the surface acidity of the MS support increased the reactivity. Compared with normal allylic alcohol, substituted allylic alcohols can be activated by surface acid sites to a greater extent. FT-IR analysis of pyridine adsorbed catalysts revealed the immobilization of Pd complex on the Brönsted acid site, resulting the presence of Pd complex close to the surface Lewis acidic

Al site. This Pd complex-Lewis acid combination should promote the concerted activation of allylic alcohols. This is the first report concerted catalysis on surface and which contribute to not only highly efficient organic synthesis but also precise design of multifunctional solid surface.

Acknowledgements

We thank Prof. Izuru Kawamura (Yokohama National University) for solid-state NMR measurements. This study was supported by the Japan Society for the Promotion of Science Grant-in-Aid for Scientific Research on Innovative Technology (Grant No. JP20H04804), Transformative Research Areas (Grant No. JP21H05099), Grant-in-Aid for Scientific Research (B) (Grant No. JP22H01863), and JST SPRING (Grant No. JPMJSP2106). XAFS was conducted with the approval of the Photon Factory Advisory Committee (Proposal Nos. 2020G033 and 2022G033).

References

1 a) Tsuji, J.; Takahashi, H.; Morikawa, M. Organic syntheses by means of noble metal compounds XVII. Reaction of π-allylpalladium chloride with nucleophiles. *Tetrahedron Lett.* **1965**, *6*, 4387-4388. b) Trost, B. M.; Fullerton, T. J. New synthetic reactions. Allylic alkylation. *J. Am. Chem. Soc.* **1973**, *95*, 292-294.

2 For reviews: a) Butt, N. A.; Zhang, W. Transition metal-catalyzed allylic substitution reactions with unactivated allylic substrates. *Chem. Soc. Rev.* **2015**, *44*, 7929-7967; b) Sundararaju, B.; Achard, M.; Bruneau, C. Transition metal catalyzed nucleophilic allylic substitution: activation of allylic alcohols via π-allylic species. *Chem. Soc. Rev.* **2012**, *41*, 4467-4483; c) Trost, B. M.; Vranken, D. L. Van Asymmetric Transition Metal-Catalyzed Allylic Alkylations. *Chem. Rev.* **1996**, *96*, 395-422; d) Trost, B. M.; Crawley, M. L. Asymmetric Transition-Metal-Catalyzed Allylic Alkylations: Applications in Total Synthesis. *Chem. Rev.* **2003**, *103*, 2921-2943; e) Lu, Z.; Ma, S. Metal-Catalyzed Enantioselective Allylation in Asymmetric Synthesis. *Angew. Chem. Int. Ed.* **2008**, *47*, 258-297; f) Lu, Z.; Ma, S. Metallkatalysierte enantioselektive Allylierungen in der asymmetrischen Synthese. *Angew. Chem.* **2008**, *120*, 264-303.

3 a) Uozumi, Y. Palladium Catalysis in Water: Design, Preparation, and Use of Amphiphilic Resin-Supported Palladium-Phosphine Complexes. *J. Synth. Org. Chem., Jpn.* **2002**, *60*, 1063-1068; b) Uozumi, Y.; Danjo, H.; Hayashi, T. New amphiphilic palladium-phosphine complexes bound to solid supports: Preparation and use for catalytic allylic substitution in aqueous media. *Tetrahedron Lett.* **1997**, *38*, 3557-3560; c) Danjo, H.; Tanaka, D.; Hayashi, T.; Uozumi, Y. Allylic substitution in water catalyzed by amphiphilic resin-supported palladium-phosphine complexes. *Tetrahedron*

1999, *55*, 14341-14352; d) Uozumi, Y.; Danjo, H.; Hayashi, T. Cross-Coupling of Aryl Halides and Allyl Acetates with Arylboron Reagents in Water Using an Amphiphilic Resin-Supported Palladium Catalyst. *J. Org. Chem.* **1999**, *64*, 3384-3388; e) Uozumi, Y.; Shibatomi, K. Catalytic Asymmetric Allylic Alkylation in Water with a Recyclable Amphiphilic Resin-Supported P,N-Chelating Palladium Complex. *J. Am. Chem. Soc.* **2001,** *123,* 2919-2920; f) Uozumi, Y.; Tanaka, H.; Shibatomi, K. Asymmetric Allylic Amination in Water Catalyzed by an Amphiphilic Resin-Supported Chiral Palladium Complex. *Org. Lett.* **2004**, *6*, 281-283; g) Uozumi, Y.; Kimura, M. Asymmetric π-allylic etherification of cycloalkenyl esters with phenols in water using a resin-supported chiral palladium complex. *Tetrahedron: Asymmetry* **2006**, *17*, 161-166; h) Kobayashi, Y.; Tanaka, D.; Danjo, H.; Uozumi, Y. A Combinatorial Approach to Heterogeneous Asymmetric Aquacatalysis with Amphiphilic Polymer-Supported Chiral Phosphine-Palladium Complexes. *Adv. Synth. Catal.* **2006**, *348*, 1561-1566; i) Uozumi, Y.; Suzuka, T.; Kawade, R.; Takenaka, H. π-Allylic Azidation in Water with an Amphiphilic Resin-Supported Palladium-Phosphine Complex. *Synlett* **2006**, 2109-2113; j) Uozumi, Y.; Suzuka, T. π-Allylic C1-Substitution in Water with Nitromethane Using Amphiphilic Resin-Supported Palladium Complexes. *J. Org. Chem.* **2006**, *71*, 8644-8646; k) Uozumi, Y. Asymmetric allylic substitution of cycloalkenyl esters in water with an amphiphilic resin-supported chiral palladium complex. *Pure Appl. Chem.* **2007**, *79*, 1481-1489; l) Uozumi, Y.; Takenaka, H.; Suzuka, T. Allylic Substitution of meso-1,4-Diacetoxycycloalkenes in Water with an Amphiphilic Resin-Supported Chiral Palladium Complex. *Synlett* **2008**, 1557-1561; m) Uozumi, Y.; Suzuka, T. π-Allylic Sulfonylation in Water with Amphiphilic Resin-Supported Palladium-Phosphine Complexes. *Synthesis* **2008**, 1960-1964; n) Yamada, Y. M. A.; Sarkar, S. M.; Uozumi, Y. Self-Assembled

Poly(imidazole-palladium): Highly Active, Reusable Catalyst at Parts per Million to Parts per Billion Levels. *J. Am. Chem. Soc.* **2012**, *134*, 3190-3198; o) Sarkar, S. M.; Uozumi, Y.; Yamada, Y. M. A. A Highly Active and Reusable Self-Assembled Poly(Imidazole/ Palladium) Catalyst: Allylic Arylation/Alkenylation. *Angew. Chem. Int. Ed.* **2011**, *50*, 9437-9441.

4 a) Kubota Y., Goto K., Miyata S., Goto Y., Fukushima Y., Sugi Y. Enhanced Effect of Mesoporous Silica on Base-Catalyzed Aldol Reaction. *Chem. Lett.* **2003**, *32*, 234-235; b) Kim K. C., Moschetta E. G., Jones C. W., Jang S. S. Molecular Dynamics Simulations of Aldol Condensation Catalyzed by Alkylamine-Functionalized Crystalline Silica Surfaces. *J. Am. Chem. Soc.* **2016**, *138*, 7664-7672; c) Brunelli N. A., Jones C. W. Tuning acid-base cooperativity to create next generation silica-supported organocatalysts. *J. Catal.* **2013**, *308*, 60-72; d) Brunelli N. A., Didas S. A., Venkatasubbaiah K., Jones C. W. Tuning Cooperativity by Controlling the Linker Length of Silica-Supported Amines in Catalysis and CO_2 Capture. *J. Am. Chem. Soc.* **2012**, *134*, 13950-13953; e) Bass J. D., Solovyov A., Pascall A. J., Katz A. Acid-Base Bifunctional and Dieletric Outer-Sphere Effects in Heterogeneous Catalysis: A Comparative Investigation of Model Primary Amine Catalysts. *J. Am. Chem. Soc.* **2006**, *128*, 3737-3747.

5 a) Ding, S.; Motokura, K. Heterogeneous Supported Palladium Catalysts for Liquid-Phase Allylation of Nucleophiles. *ChemPlusChem* **2020**, *85*, 2428-2437; b) Noda, H.; Motokura, K.; Miyaji, A.; Baba, T. Heterogeneous Synergistic Catalysis by a Palladium Complex and an Amine on a Silica Surface for Acceleration of the Tsuji–Trost Reaction. *Angew. Chem. Int. Ed.* **2012**, *51*, 8017–8020; *Angew. Chem.* **2012**, *124*, 8141–

8144; c) Noda, H.; Motokura, K.; Miyaji, A.; Baba, T. Efficient Allylation of Nucleophiles Catalyzed by a Bifunctional Heterogeneous Palladium Complex-Tertiary Amine System. *Adv. Synth. Catal.* **2013**, *355*, 973–980; d) Motokura, K.; Saitoh, K.; Noda, H.; Chun, W.-J.; Miyaji, A.; Yamaguchi, S.; Baba, T. A Pd–bisphosphine complex and organic functionalities immobilized on the same SiO_2 surface: detailed characterization and its use as an efficient catalyst for allylation. *Catal. Sci. Technol.* **2016**, *6*, 5380–5388; e) Motokura, K.; Saitoh, K.; Noda, H.; Uemura, Y.; Chun, W.-J.; Miyaji, A.; Yamaguchi, S.; Baba, T. Co-Immobilization of a Palladium–Bisphosphine Complex and Strong Organic Base on a Silica Surface for Heterogeneous Synergistic Catalysis. *ChemCatChem* **2016**, *8*, 331–335; f) Motokura, K.; Ikeda, M.; Kim, M.; Nakajima, K.; Kawashima, S.; Nambo, M.; Chun, W.-J.; Tanaka, S. Silica Support-Enhanced Pd-Catalyzed Allylation Using Allylic Alcohols. *ChemCatChem* **2018**, *10*, 4536–4544; g) Motokura, K.; Kawashima, S.; Nambo, M.; Manaka, Y.; Chun, W.-J.; Accumulation of Active Species in Silica Mesopore: Effect of the Pore Size and Free Base Additives on Pd-catalyzed Allylation using Allylic Alcohol. *ChemCatChem* **2020**, *12*, 2783–2791.

6 a) Ozawa, F.; Okamoto, H.; Kawagishi, S.; Yamamoto, S.; Minami, T.; Yoshifuji, M. (π-Allyl)palladium Complexes Bearing Diphosphinidenecyclobutene Ligands (DPCB): Highly Active Catalysts for Direct Conversion of Allylic Alcohols. *J. Am. Chem. Soc.* **2002**, *124*, 10968; b) Manabe, K.; Kobayashi, S. Palladium-Catalyzed, Carboxylic Acid-Assisted Allylic Substitution of Carbon Nucleophiles with Allyl Alcohols as Allylating Agents in Water. *Org. Lett.* **2003**, *5*, 3241; c) Kinoshita, H.; Shinokubo, H.; Oshima, K. Water Enables Direct Use of Allyl Alcohol for Tsuji−Trost Reaction without Activators. *Org. Lett.* **2004**, *6*, 4085; d) Patil, N. T.; Yamamoto, Y.; Direct allylic substitution of

allyl alcohols by carbon pronucleophiles in the presence of a palladium/carboxylic acid catalyst under neat conditions. *Tetrahedron Lett.* **2004**, *45*, 3101; e) Yang, S.-C.; Hsu, Y.-C.; Gan, K.-H. Direct palladium/carboxylic acid-catalyzed allylation of anilines with allylic alcohols in water. *Tetrahedron* **2006**, *62*, 3949-3958; f) Usui, I.; Schmidt, S.; Keller, M.; Breit, B. Allylation of *N*-Heterocycles with Allylic Alcohols Employing Self-Assembling Palladium Phosphane Catalysts. *Org. Lett.* **2008**, *10*, 1207-1210; g) Usui, I.; Schmidt, S.; Breit, B. Dual Palladium- and Proline-Catalyzed Allylic Alkylation of Enolizable Ketones and Aldehydes with Allylic Alcohols. *Org. Lett.* **2009**, *11*, 1453-1456; h) Jiang, G.; List, B. Direct Asymmetric α-Allylation of Aldehydes with Simple Allylic Alcohols Enabled by the Concerted Action of Three Different Catalysts. *Angew. Chem. Int. Ed.* **2011**, *50*, 9471-9474; i) Tao, Z.-L.; Zhang, W.-Q.; Chen, D.- F.; Adele, A.; Gong, L.-Z. Pd-Catalyzed Asymmetric Allylic Alkylation of Pyrazol-5-ones with Allylic Alcohols: The Role of the Chiral Phosphoric Acid in C–O Bond Cleavage and Stereocontrol. *J. Am. Chem. Soc.* **2013**, *135*, 9255-9258; j) Zhou, H.; Yang, H.; Liu, M.; Xia, C.; Jiang, G. Brønsted Acid Accelerated Pd-Catalyzed Direct Asymmetric Allylic Alkylation of Azlactones with Simple Allylic Alcohols: A Practical Access to Quaternary Allylic Amino Acid Derivatives. *Org. Lett.* **2014**, *16*, 5350-5353; k) Banerjee, D.; Junge, K.; Beller, M. Cooperative Catalysis by Palladium and a Chiral Phosphoric Acid: Enantioselective Amination of Racemic Allylic Alcohols. *Angew. Chem. Int. Ed.* **2014**, *53*, 13049-13053; l) Gumrukcu, Y.; De Bruin, B.; Reek, J. N. H. Hydrogen-Bond-Assisted Activation of Allylic Alcohols for Palladium-Catalyzed Coupling Reactions. *ChemSusChem* **2014**, *7*, 890-896; m) Huo, X.; Yang, G.; Liu, D.; Liu, Y.; Gridnev, I. D.; Zhang, W. Palladium-Catalyzed Allylic Alkylation of Simple

Ketones with Allylic Alcohols and Its Mechanistic Study. *Angew. Chem. Int. Ed.* **2014**, *53*, 6776-6780.

7 a) Kolodziejski W.; Corma, A.; Navarro, M.-T.; Pérez-Pariente, J. Solid-state NMR study of ordered mesoporous aluminosilicate MCM-41 synthesized on a liquid-crystal template. *Solid State Nucl. Magn. Reson.* **1993**, *2*, 253-259. b) Reddy, K. M.; Song, C. Synthesis of mesoporous molecular sieves: influence of aluminum source on Al incorporation in MCM-41. *Catal. Lett.* **1996**, *36*, 103-109.

8 a) Kosslick, H.; Lischke, G.; Parlitz, Storek, B. W.; Fricke, R. Acidity and active sites of Al-MCM-41. *Appl. Catal. A: Gen.* **1999**, *184*, 49-60. b) Chakraborty, B.; Viswanathan, B.; *Catal. Today* **1999**, *49*, 253-260. c) Sedran, U.; Fígoli, N. Acidity modification by thermal and steam treatment in silica-alumina and its relation with methanol to hydrocarbons reaction. *React. Kinet. Catal. Lett.* **1989**, *39*, 363-366. d) Yamaguchi, S.; Yabushita, M.; Kim, M.; Hirayama, J.; Motokura, K.; Fukuoka, A.; Nakajima, K. Catalytic Conversion of Biomass-Derived Carbohydrates to Methyl Lactate by Acid–Base Bifunctional γ-Al_2O_3. *ACS Sustainable Chem. Eng.* **2018**, *6*, 8113-8117.

9 Moschetta E.G., Brunelli N. A., Jones C. W. Reaction-dependent heteroatom modification of acid-base catalytic cooperativity in aminosilica materials. *Appl. Catal. A-Gen.* **2015**, *504*, 429-439.

10 Tanev, P. T.; Pinnavaia, T. J. A Neutral Templating Route to Mesoporous Molecular Sieves. *Science* **1995**, *267*, 865-867.

11 Motokura, K.; Ikeda, M.; Nambo, M.; Chun, W.-J.; Nakajima, K.; Tanaka, S. Concerted Catalysis in Tight Spaces: Palladium-Catalyzed Allylation Reactions Accelerated by Accumulated Active Sites in Mesoporous Silica. *ChemCatChem* **2017**, *9*, 2924-2929.

12 Daasch, L. W.; SMITH, D. C. Infrared Spectra of Phosphorus Compounds. *Anal. Chem.* **1951**, *23*, 853-868.

13 Klinowski, J.; Thomas, J. M.; Fyfe, C. A.; Gobbi, G. C. Monitoring of structural changes accompanying ultrastabilization of faujasitic zeolite catalysts. *Nature* **1982**, *296*, 533-536.

14 Corrêa, R. S.; Graminha, A. E.; Ellena, J.; Batista, A. A. Weak C-H···Cl-Pd inter-actions toward conformational polymorphism in trans-di-chloridobis-(tri-phenyl-phosphane)palladium(II). *Acta Cryst.* **2011**, *C67*, m304-306.

15 Parry, E. P.; An infrared study of pyridine adsorbed on acidic solids. Characterization of surface acidity. *J. Catal.* **1963**, *2*, 371-379.

16 Busca, G. The surface acidity of solid oxides and its characterization by IR spectroscopic methods. An attempt at systematization. *Phys. Chem. Chem. Phys.*, **1999**, *1*, 723-736.